

**UHASSELT**



**Maastricht University**

KNOWLEDGE IN ACTION

**Faculty of Medicine and Life Sciences**  
**School for Life Sciences**

Master of Biomedical Sciences

**Master's thesis**

**Cartilage mineralization; the adverse effects of calcium-containing crystals and VEGFa on human OA articular chondrocytes**

**Michael Stouten**

Thesis presented in fulfillment of the requirements for the degree of Master of Biomedical Sciences, specialization Environmental Health Sciences

**SUPERVISOR :**

Dr. Guus VAN DEN AKKER

**MENTOR :**

MSc. Roderick STASSEN

Transnational University Limburg is a unique collaboration of two universities in two countries: the University of Hasselt and Maastricht University.



**UHASSELT**

KNOWLEDGE IN ACTION

[www.uhasselt.be](http://www.uhasselt.be)  
Universiteit Hasselt  
Campus Hasselt:  
Martelarenlaan 42 | 3500 Hasselt  
Campus Diepenbeek:  
Agoralaan Gebouw D | 3590 Diepenbeek

**2022**  
**2023**



**Maastricht University**

# **Faculty of Medicine and Life Sciences**

## ***School for Life Sciences***

Master of Biomedical Sciences

### ***Master's thesis***

***Cartilage mineralization; the adverse effects of calcium-containing crystals and VEGFa on human OA articular chondrocytes***

**Michael Stouten**

Thesis presented in fulfillment of the requirements for the degree of Master of Biomedical Sciences, specialization Environmental Health Sciences

### **SUPERVISOR :**

Dr. Guus VAN DEN AKKER

### **MENTOR :**

MSc. Roderick STASSEN



## Cartilage mineralization; the adverse effects of calcium-containing crystals and VEGFa on human OA articular chondrocytes

Michael Stouten, Roderick Stassen<sup>1</sup>, and Guus Van Den Akker<sup>1</sup>

<sup>1</sup>Laboratory for Experimental Orthopedics, Department of Orthopedic Surgery, Maastricht University, Universiteitssingel 50, 6229 ER Maastricht, The Netherlands.

\*Running title: *Characterisation of driving factors in osteoarthritis*

To whom correspondence should be addressed: Guus Van Den Akker, Tel: +31-43-3881531; Email: g.vandenakker@maastrichtuniversity.nl

**Keywords:** Osteoarthritis; Mineralization; Crystals; VEGF

### ABSTRACT

**Background:** Cartilage mineralization arises as calcium-containing particles (CCP) precipitation in the degenerated articular cartilage of osteoarthritis (OA). However, it is unclear how crystal formation occurs and whether these crystals are a disease driver or a response. Therefore, we aim to investigate the effects of CCPs on human OA chondrocytes (HACs). Since vascular endothelial growth factor was increased in OA synovial fluid, we aim to study the role of VEGFa as an inducer of mineralization.

**Method:** Prepared primary (pCPP), secondary (sCPP) calciprotein particles and basic calcium phosphate (BCP) crystals were evaluated for their physiological relevance by TEM, NTA and colorimetric assays. The CCPs were exposed to OA-HACs to study by RT-qPCR and ELISA. The bioactivity of VEGFa was evaluated in chondrocytes and studied for mineralization induction in a phosphate-induced OA-HAC model by colorimetric assays.

**Results:** Synthesized pCPP, sCPP and BCP were confirmed as physiological based on morphology, size and chemical content. These particles demonstrated a particle-induced stress reaction and induction of IL-6, CXCL-8, COX-2, MMP-1 and VEGFA expressions and IL-6, CXCL-8 and PGE2 secretions in OA-HACs. Bio-activity of 100ng/mL VEGFa was demonstrated in chondrocytes for IL-6 secretions. The same concentration of VEGFa induced an increased crystal formation in OA-HACs.

**Conclusion:** The CPPs induced an aberrant chondrocyte phenotype in OA-HACs. VEGFa was indicated to be an inducer of

**mineralization and crystal formation in OA-HACs. These results give an understanding of the mechanisms behind the role of CCPs and VEGFa mineralization in OA, which aid in the development of new therapeutic insights.**

### INTRODUCTION

Osteoarthritis (OA) is the most prevalent degenerative joint disease in arthritis causing disability among middle-aged and older adults worldwide (1). Patients suffer mainly from stiffness, chronic pain and impaired mobility due to direct bone-to-bone contact, instability, deformation and narrowing of the articular joints (Figure 1) (2). Furthermore, the disease is characterized by the degradation of the articular cartilage, synovial inflammation and changes in the subchondral bone, synovium, menisci and ligaments (Figure 1) (3, 4). Large weight-bearing joints, such as hips, knees, ankles and the facet joints in the spine are the most frequently affected (3, 5). In the last decades, OA was considered a simple disease of “wear and tear”, but nowadays OA is defined as a multifactorial pathology as a result of physical immobility, sedentary lifestyle, life expectancy, sports injuries and BMI (6, 7). Due to an increase in the risk factors, the prevalence of OA is continuously rising and is expected to increase even further (4). According to the Global Burden of Disease 2010 study, the disease is already reported as the 11th highest contributor to global disability out of 291 diseases, with an increasing prevalence of more than 500 million people in 2019 (8, 9). OA affects 9.6% of men and 18% of women over the age of 60 years (6, 10). However, also athletes and younger individuals are affected by joint traumas after persistent physical activities (11). Additionally, OA is associated with an increased

mortality rate compared to the general population, in which disability is demonstrated as a significant predictor of survival (6). Since the burden of the disease is rising globally, the socioeconomic burden will further increase due to direct healthcare costs and indirect costs from living with this disabling condition (10). In general, OA is diagnosed after the awareness of continuous joint pain, physical examination and radiographic evidence, though some patients are asymptomatic (4). The disease can be treated for its symptoms via physical activity and pharmacological modalities. Due to the complexity of the pathology, no preventable or reversible therapy exists. Currently, only arthroplasty, including total joint replacement by metal and plastic prosthesis, is performed to treat the disease. Since OA still cannot be cured, the different aspects of the disease should be more elaborated in scientific research.

non-collagenous proteins residing in a limited number of chondrocytes. Together, these components induce water retention to maintain unique mobility properties (13). Although these chondrocytes consist of only 5% of the total volume of the articular cartilage, they orchestrate the overall maintenance and repair of the ECM via collagens and proteoglycans synthesis (12, 13). The major fibrillar collagens consist of collagen type II, but also minor groups of collagen types are present such as type I, IV, V, VI, IX and XI. These minor types are necessary to stabilize the fibril network of type II collagens via cross-links and binding with the proteoglycan aggregates. Additionally, hyaline cartilage is defined by aggrecan, a highly glycosylated protein mainly expressed by chondrocytes (13). Aggrecan consists of chondroitin sulphate and keratin sulphate chains both composed of repeating disaccharide subunits with sulphate groups. These sulphate groups induce an overall negative charge to attract cations within the matrix and increase the osmolality of the tissue, which in turn attracts water. As a consequence, the osmolality decreases again. Therefore, articular cartilage has a higher tissue pressure than other tissues do, but due to the type II collagen interconnections, swelling is prevented; resulting in the unique mechanical properties of articular cartilage.

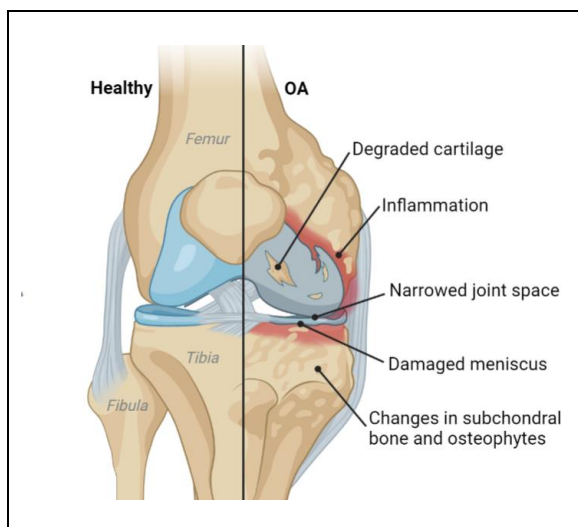


**Figure 1: Medial side of the healthy and OA knee.** The OA knee is affected by degradation of the articular cartilage, synovial inflammation, narrowed joint space, damaged meniscus and osteophytes. OA; osteoarthritis. Figure created with BioRender (<https://biorender.com/>).

The most prominent feature of OA is the degeneration of the articular cartilage (Figure 1). This articular cartilage is defined as a highly specialised, smooth and lubricated connective tissue at the diarthrodial joints (12). This type of tissue is able to minimise compressive forces and friction for better articulation of the joints and mobility. Furthermore, this hyaline cartilage is composed of a dense extracellular matrix (ECM) of glycoproteins, proteoglycans, collagen and

Nevertheless, articular cartilage is limited in repair mechanisms due to a lack of innervation, vascularization and lymphatics (14). As a result, chondrocytes have a slow replicative capacity making the tissue more susceptible to deficiencies and pathologies. In OA, this can lead to mineralization of the articular cartilage by deposition of calcium-containing crystals in the ECM of the articular cartilage, but also in the synovial fluid, leading to tissue degeneration (15). However, mineralization in general is not a pathological event. Endochondral ossification (EO), the development of long bones, occurs through a physiological mineralization process (16, 17). This ossification process initiates with the condensation of lateral plate mesenchymal cells to the places of the future bones (17, 18). These cells differentiate into chondrocytes and start secreting type II collagen and aggrecan rich-matrix to form cartilage (16, 17). Eventually, this cartilage enlarges through chondrocyte proliferation and matrix production, but at the end of the cartilage mould, the chondrocytes stop dividing and enlarge to become hypertrophic.

These hypertrophic chondrocytes alter the ECM matrix by producing type X collagen and fibronectin to enable cartilage mineralization by crystals such as calcium carbonate (16). Eventually, the hypertrophic chondrocytes die and osteoblasts around the cartilage mould form a bone matrix on the partially degraded cartilage. At the joint ends, the articular cartilage is unaffected throughout life residing chondrocytes in a non-proliferating resting phase (19). The crystal precipitation in articular cartilage during OA occurs similarly to the hypertrophy of growth plate chondrocytes. In the pathological state, chondrocytes quit their resting phase and enter an EO-like sequence of proliferation, hypertrophic differentiation, apoptosis and mineralization of the diseased articular cartilage. This hypertrophic differentiation is featured by the increased metabolic activity of the chondrocytes resulting in an altering synthesis of ECM molecules and proteases. This state is associated with the expression of alkaline phosphatase, collagen X and MMP-13 leading to impaired homeostasis and degeneration of the cartilage tissue.

Less is known about the actual driving forces of hypertrophic differentiation in OA. It has been known that cartilage homeostasis is influenced by mechanical load, the surrounding matrix, cytokines, growth factors, ageing and injury; factors that can impact tissue integrity (12, 13). During the regulation of EO, several locally expressed growth factors are present such as morphogenetic proteins (BMPs), fibroblast growth factors (FGFs), transforming growth factor  $\beta$  (TGF- $\beta$ ), Indian hedgehog (IHH) and Wntless/Integrated (Wnt) (19). For example, active TGF- $\beta$  differs in concentration levels between healthy and OA joints (20). High amounts of TGF- $\beta$  are stored in the ECM of articular cartilage but in an inactive form. Upon mechanical loading, these inactive TGF- $\beta$ s release their latency-binding peptide to become activated. Regular loading is necessary to keep the cartilage vital. Although, constant elevated levels of active TGF- $\beta$  are present in OA leading to an altered activation of the chondrocytes and their pathways. This aligns with preliminary data from our group, in which spontaneous mineralization occurs upon exposure to high concentrations of TGF- $\beta$  to OA-human articular chondrocytes (HAC). A TGF- $\beta$  target gene, vascular endothelial growth factor (VEGF), is known for its angiogenic properties and is important for neonatal bone formation during EO

(21). However, the VEGF/VEGFR expression is usually not found in the healthy human articular cartilage of adults. Although, VEGF/VEGFR has been reported to be present in high concentrations in OA. Therefore, VEGFA has been suspected to be an inducer of crystal formation in articular cartilage mineralization since the growth factor trigger vascularisation, as a source of calcium and phosphate. Fewer studies describe the mineralization-inducing capacity of growth factors and therefore the influence of growth factors, such as VEGF, on mineralization needs to be further elucidated.

At the moment of total knee replacement surgery, calcium-containing crystals are found in the synovial fluid and in the tissue of affected joints of all OA patients (22). The major crystals found in OA are basic calcium phosphate (BCP) and calcium pyrophosphate deposition (CPPD) crystals (23). Although pathological mineralization is correlated with the extent of joint destruction and the disease progression, it is unclear whether these crystals are either a driver or a result of the disease (24). However, the BCPs include a heterogeneous group of crystalline non-acidic calcium phosphates such as hydroxyapatite (HA) and to a lesser extent octacalcium phosphate, tricalcium phosphate and whitlockite (15, 23, 24). Although, the formation of crystals is a physiological process and is still under debate. One of the concepts for crystal formation is the presence of Posner's clusters in body fluids (25). These clusters consist of supersaturated calcium and phosphate ions and are able to agglomerate to form amorphous calcium phosphate (ACP), a precursor of HA (Figure 2A). Eventually, different ACPs cluster and form pure HA. Nonetheless, the conversion of ACP to HA occurs over an extended period of time, resulting in the formation of precursors. These precursors are known as calciprotein particles (CPP) (26). The primary CPPs (pCPP) rearrange to more stable secondary CPPs (sCPP) and are characterized by the binding of liver-derived fetuin-A proteins (27). In physiological conditions, fetuin-A proteins limit changing calcium and phosphate homeostasis over time and ensure adequate mineralization at the right place and time. Fetuin-A binds calcium and phosphate over several orders of scale. Moreover, fetuin-A's gene, AHSG, has been found in higher abundance in OA synovial fluid compared to non-OA synovial fluid, suggesting an increase in crystal presence and formation in OA (28). Besides, it

has been known that the precipitation of these BCPs is regulated by the ratio of phosphate (Pi) to inorganic pyrophosphate (PPi) (Figure 2B) (23). At physiological concentrations, PPi inhibits mineralization and suppresses the synthesis of HA crystals, while excessive Pi levels promote BCP formation. Therefore, a balance of Pi and PPi is regulated by chondrocytes to prevent pathological mineralization in cartilage tissue. This balance is monitored by several transmembrane enzymes, such as tissue-nonspecific alkaline phosphatase (TNAP), the multiple pass transmembrane protein Ankryn (ANK) and nucleotide pyrophosphatase phosphodiesterase (NPP1) (Figure 2C). NNPI generates PPi via the cleavage of ATP, ANK transports intracellular PPi across the cell membrane, while TRAP antagonises NPP1 by hydrolysing PPi to Pi. Nevertheless, the precipitation of calcium-containing crystals in OA joints is pathological and is suggested to be due to an aberrant chondrocyte phenotype favouring hypertrophy and mineralization (19). Since BCPs induce synovial inflammation, cartilage degradation and expression of matrix-degrading genes in knee joints of mice after injection, the impact of BCPs and its precursors on OA chondrocytes are investigated (29).

articular cartilage in OA. However, it is unclear which factors induce the loss of chondrocyte phenotypic integrity that leads to the pathological formation of these crystals. Therefore, we aimed to investigate the potential impact of driving factors on these chondrocytes. Since it is unknown whether the crystals are a disease driver or a response, our research considered these crystals as potential inducers of these hypertrophic chondrocytes. Therefore, we hypothesized that the presence of pCPP, sCPP and BCP will impact the chondrocytes' behaviour, with respect to cell morphology and changes in expression patterns of genes and proteins. During an *in vitro* experiment, OA-HACs will be exposed to different crystals to study subsequent changes in gene and protein levels. Furthermore, differential expression of VEGF at the gene or protein level is suggested to have a role in the pathological mineralization of OA HACs. Therefore, we hypothesize that VEGFa increases phosphate-induced (PI) OA-HAC mineralization. Our research group developed an *in vitro* PI mineralization model to study the impacts of growth factors on mineralization. Altogether, this research will provide insight into the mechanisms behind the role of VEGF on mineralization and the effects of crystals on OA-HACs.

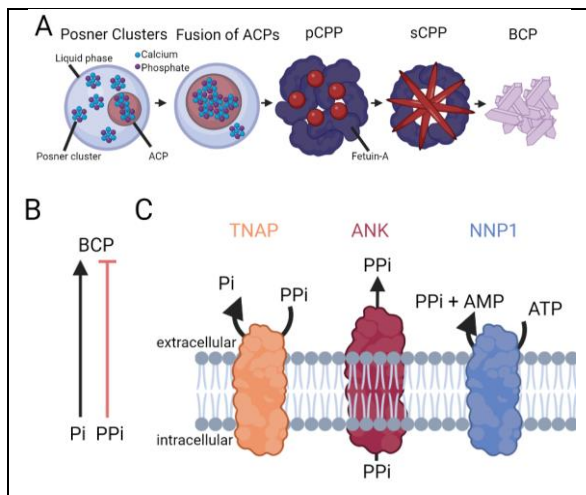


**Figure 2: Crystal formation.** A) Formation of pCPP, sCPPs and BCPs. B) Balance of Pi and PPi. C) Enzymes coordinating the Pi/PPi ratio. BCP, basic calcium phosphate; Pi, phosphate; PPi, inorganic phosphate; pCPP and sCPP, primary and secondary calciprotein particle; BCP, Basic calcium phosphate. Figure created with BioRender (<https://biorender.com/>).

## EXPERIMENTAL PROCEDURES

**Isolation and culturing** – Different cell types were used during the experiments; C28I2 human chondrocyte cell line (ATCC) and OA-HACs. OA-HACs were isolated from surgical waste material from total knee replacement surgeries performed on end-stage OA patients at the Maastricht University Medical Center+ and the Sint-Annadal Hospital in the Netherlands. Ethical approval was obtained from the local ethical committee with approval identification: METC 2017-0183. Subsequently, cartilage tissue was cut from all the parts of the femur and incubated overnight on 1:10 collagenase type II (Invitrogen). After incubation, the digested cartilage was filtered for OA-HACs with a 70µm cell strainer and cultured until passage 1 in DMEM/F12 Low glucose & GlutaMAX (Gibco), containing 10% fetal calf serum (FCS) (Sigma-Aldrich), 1% antibiotic/antimitotic 100x (P/S) (Gibco) and 1% non-essential amino acids (NEAA) (Gibco) under a humidified atmosphere of 37° C and 5% CO<sub>2</sub>. Two different pools of respectively 6 and 8 OA-HAC donors were used at the second passage for further experiments

The aberrant chondrocyte phenotype is considered a driver of the mineralization of

(Supplementary Table 1). The C28I2 cell line was cultured under the same conditions but without the 1% NEAA (Gibco) medium supplement. Both cell types were seeded at a density of 30 000 cells/cm<sup>2</sup> and allowed for attachment for 24 hours before the start of the experiment.

*Crystal synthesis, characterization and impact* – The BCPs were prepared by alkaline hydrolysis of brushite (30). This was performed by slowly adding 0.2M sodium phosphate buffer to 0.2M CaCl<sub>2</sub>. After 1 hour of stirring at room temperature, the precipitate was centrifuged at low speed and discarded for the supernatant. After washing, 0.5M HCl and 20% NaOH to adjust the pH to 8.5. pCPPs and sCPPs were generated by adding 10% FCS (Sigma-Aldrich), 3.5mM inorganic phosphate, 1mM calcium, 1% P/S (Gibco), and 1% L-Glutamine (Gibco) to phenol-red free DMEM (Gibco) (28). This calcification medium was stored at 37°C for either 1 or 7 days to develop pCPPs and sCPPs, respectively. The solution was centrifuged at 21 380xg for 120 minutes at 4°C to pellet the pCPPs and sCPPs. The different crystals were resuspended for a final concentration of 50µg/mL. Characterization of the different crystals was performed with Transmission Electron Microscopy (TEM) (Tecnai) and with the Zetaview® Nanoparticle Tracking Analysis (NTA) (Analytik). TEM performed an imaging of the morphological features at 2µm and 50nm. The crystals were applied on a grid of nickel for drying at room temperature and visualized without staining from 2µm to 50nm. The NTA used light scattering and the Brownian motion to analyse the size distribution of the particles within the range of 10nm to 1000nm. To assess the impact of the different crystals on the protein and gene levels of chondrocytes, an OA-HAC pool of 6 patients (Supplementary Table 1) was cultured. The culture media were prepared with DMEM/F12 Low glucose & GlutaMAX (Gibco), containing 10% FCS (Sigma-Aldrich), 1% P/S (Gibco) and 1% NEAA supplemented with 50µg/mL of BCPs, sCPPs or sCPPs. The different conditions were followed up over time with light microscopy (Zeiss) after 0, 24 and 48 hours at 20 and 100µm. The media were collected for ELISA. The wells were washed with 0.9% NaCl for further procedures with RT-qPCR.

*The bioactivity and mineralization capacity of VEGF* – C28I2 cells were cultured in DMEM (Gibco) with 10% FCS (Gibco), 1% P/S (Gibco)

supplemented with 50ng/mL and 100ng/mL of VEGFa (Biotechne Ltd, R&D Systems). The isoform, type A, of VEGF (VEGFa) is used since this growth factor is commonly used in scientific research for the demonstration of VEGF properties. To assess the mineralization capacity of VEGFa, a PI-OA-HAC model was used. The negative control's media consisted of 10% FCS (Gibco), 1% P/S (Gibco), and 1% NEAA (Gibco), while the positive control was complemented with 1mM ATP (New England Biolabs, Bioke) and 10mM BGP (Sigma-Aldrich). The OA-HAC pool consisted of 8 patients (Supplementary Table 1) and was cultured in the same medium as the positive control supplemented with either 10ng/mL or 100ng/mL of VEGFa. The cells were exposed to the same concentrations every two days and followed up with light microscopy (Zeiss) after 6 and 7 days of exposure at 20 and 100µm. The media were collected for ELISA and the cells were washed twice with 0.9% NaCl for the colorimetric assays.

*RNA isolation and RT-qPCR* – Chondrocytes were lysed with TRIzol™ (ThermoFisher). A phase separation of RNA and proteins was formed after the addition of (5:1) chloroform (VWR). The RNA was precipitated with (1:1) isopropanol (VWR). After 2.5h at -20°C, the precipitate was centrifuged again for 60 minutes at 4°C for 21 380xg to wash it with 80% ethanol. After the removal of the supernatant, the pellet was resuspended in RNase-free MQ water. RNA concentrations were determined by Nanodrop™ One (ThermoFisher Scientific). Complementary DNA was reverse transcribed from 216.7 RNA using reverse transcriptase (RT) mix. The RT mix of 10µL per sample was prepared with 5x RT buffer (5x) (Promega), hexamers primers (0.02µg/µL) (Promega) and dNTPs (20mM) (Eurogentec) to add to each RNA sample for the initial phase of the thermal reaction in the Biometra TRIO (Analytik Jena). The second phase was continued after the addition of the enzyme mix (EM) which contained DTTs (0.1M) (Serva), RNasin (20U/µL) (Promega) and M-MLV reverse transcriptase (200U/µL) (Promega) and MQ. The thermal reaction followed the subsequent protocol: 6 minutes at 72°C and 5 minutes at 37°C (initial phase), and 1 hours at 37°C and 5 minutes at 95°C (second phase). A PCR mix was prepared and added to the cDNA for amplification with the Bio-Rad CFX96 RT-qPCR detection system. The PCR mix consisted of Takyon NO ROX SYBR MasterMix

dTTP blue (Eurogentec), MQ, 2ng/μL of cDNA samples and reversed and forward PCR primers per sample (20μM) (Eurogentec) with an end volume of 15μL. The RT-qPCR followed the 50-cycle standard protocol: 10 minutes denaturation at 95°C, 50 amplification cycles of each 15 seconds at 95°C and 1 minute at 60°C. The used RT-qPCR primers are presented in Supplementary Table 2. The expression of the genes of interest was quantified with the standard curve method with normalization to the reference gene Cyclophilin (PPIA) (Eurogentex) following the  $\Delta\Delta C_t$  method.

*Enzyme-linked immune sorbent assay* – The culture media were collected to evaluate the protein levels with the enzyme-linked immune sorbent assay (ELISA). The absorbance of the protein concentrations of hIL-6 (R&D, DY206-05), hCXCL-8 (R&D, DY208-05) and hPGE2 (Cayman, 514010-96) was measured with the MultiSkan™ FC Microplate Photometer (ThermoFisher Scientific) according to the manufacturer's instructions. All the samples and standards were measured in duplicates.

*Colorimetric assays* – To perform the different colorimetric assays, the cells were lysed with 0.1M HCl for 2-3 hours at room temperature on a shaker. The amount of calcium was determined with the Randox assay. The Calcium Reference sample was diluted over a dilution series of 1:1.5 in 1M HCl. The samples and standard were supplemented with 1:1 CPC/AMP reagents to measure the absorbance at 560nm after an incubation of 5 minutes. In the phosphate assay (Sigma-Aldrich), the samples and standards were diluted with MQ. A 1:10 dilution series of 0.1mM phosphate standard was prepared. After adding the Phosphate Reagent to each well and 30 minutes of incubation, the absorbances were measured at 650nm. The total protein colorimetric BCA assay (ThermoFisher) used a 1:2 dilution series of the RIPA/BSA standard. Each well was supplemented with solution C, consisting of 50:1 bicinchoninic acid solution and copper(II) sulphate solution. After an incubation of 60 minutes at 37°C, the absorbance was measured at 560nm. MultiSkan™ FC Microplate Photometer (ThermoFisher Scientific) was used to measure the absorbance. All colorimetric assays were performed according to the manufacturer's protocols. All the samples and standards were measured in duplicates.

*Statistics* – Statistical analysis was performed with GraphPad Version 8.4.2. Statistical significance between the two groups was tested by a two-tailed unpaired Student's *T*-test, with a significant threshold of 5%. All statistical tests were performed according to the assumptions of normal data distribution and homogeneity of the variances. The OA-HAC pools were used to limit patient-dependent variation. The conditions were compared with the controls unless indicated differentially. The data represented in bars consisted of mean±standard deviation of the data.

**RESULTS**

*Crystal characterization* – To assess the impact of pCCP, sCCP and BCP particles on OA chondrocytes, the presence and formation of the different particles needed to be confirmed based on their morphological structure, size distribution and chemical content. The pCCPs, sCCPs and BCPs were prepared and individually analysed for their morphological characteristics with TEM and for their distribution in size with NTA. The TEM images visualized the different particles separately (Figure 3). The pCCP particles were individually distributed as perfect spherical particles, while the sCCP were clustering with

neighbouring particles (Figure 3A-B). Moreover, the sCCPs lost their perfect spherical features and demonstrated the formation of protrusions at the surface (Figure 3A-B). TEM imaging revealed a dense cluster formation of the BCPs (Figure 3C). However, TEM images with a scale bar of 100 and 50nm indicated individual BCPs demonstrating crystallinity features and layer formation of elongated rods. TEM was able to confirm the formation of the different particles and their physical characteristics. Furthermore, the size of the particles was analysed with the NTA. An average size of 144.5nm for pCCP, 143.3nm for sCCP and 123.2nm for BCP was

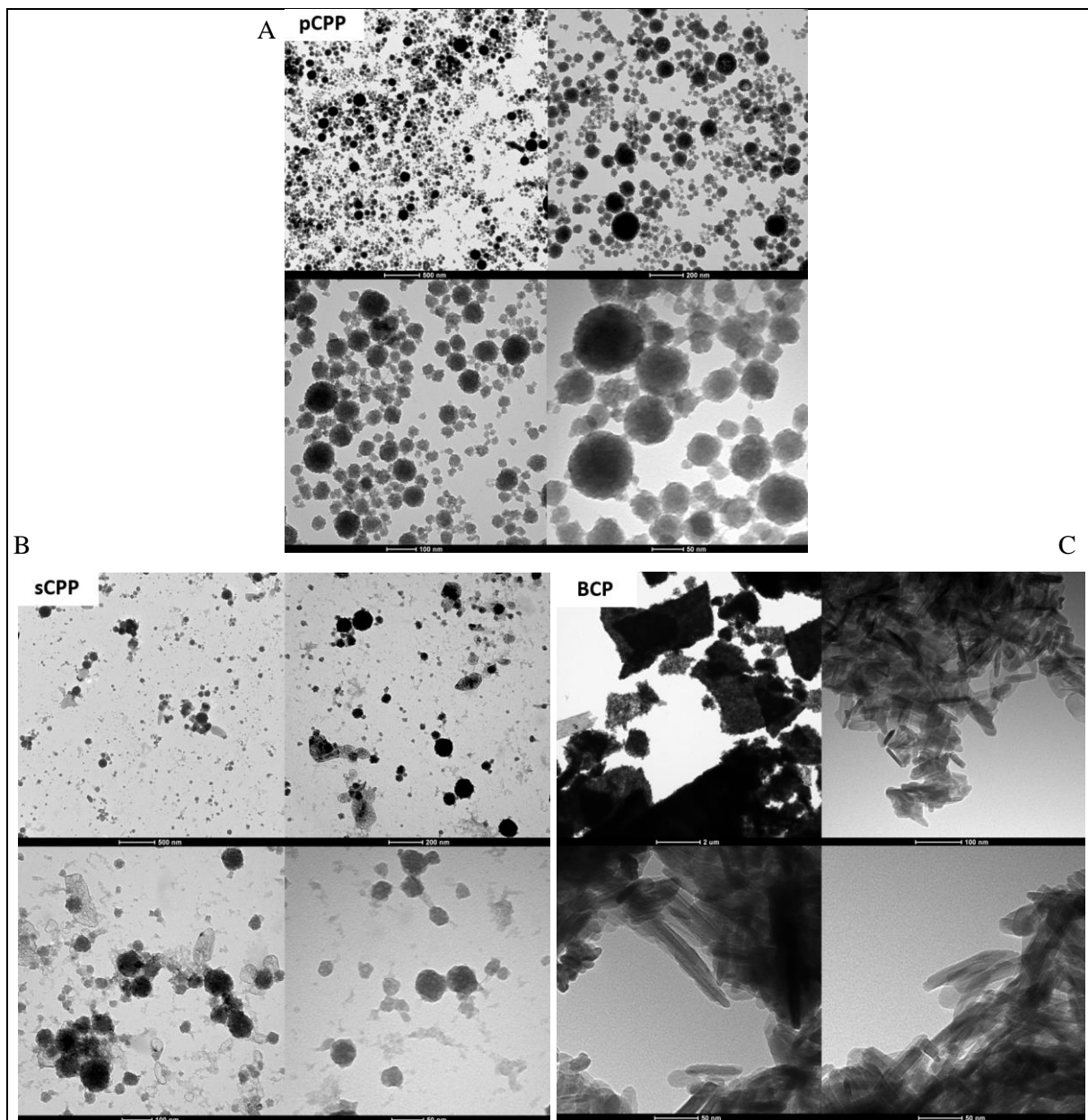


**Figure 3: TEM imaging of pCCP (A), sCCP (B) and BCP (C).** The particles were loaded on a nickel-grid at room temperature to drying and visualized without staining. pCCP, primary calciprotein particle; sCCP, secondary calciprotein particle; BCP, basic calcium phosphate; TEM, transmission electron microscopy.

measured. Moreover, the NTA visualized the distribution in size (Figure 4). The largest fraction (52%) of the pCPPs was 133.5nm in size, while the minor fraction (48%) had a diameter of 182.1nm (Figure 4A). The sCPPs had a more diverse distribution in size: 27.3% of the particles was 103.3nm, while larger fractions were 202.8nm and 142.4nm in size, 33.8% and 38.9% respectively (Figure 4B). The BCPs were more heterogeneously distributed in particle size: 132.1nm (12.2%), 265.6nm (13.8%), 50.3nm (21.4%), 99.3nm (21.7%) and 173.6nm (25.4%) in size (Figure 4C). Although there is a variation in size, the NTA was able to measure the sizes of pCPPs, sCPPs and BCPs, which were complying with previous studies (31, 32). Additionally, the particles were chemically characterized for calcium, phosphate and protein contents with colorimetric assays. The amount of calcium per particle demonstrated a significant increase in calcium concentration from pCPP to sCPP and a significant decrease from sCPP to BCP (Figure 5A). The amount of phosphate per particle indicated a significant increase in phosphate concentration from pCPP to sCPP and from sCPP to BCP (Figure 5B). Also, the amount of protein per particle determined a significant decrease from pCPP to sCPP and from sCPP to BCP (Figure 5C). These results demonstrated differences in the chemical content between the different particles. Our data indicated an increase of both calcium and phosphate contents passing from pCPP to sCPP, which was confirmed by the deposition found in generated particles studied in the calcification of vascular smooth muscle cells (30). Furthermore, low protein contents in BCPs were expected, since several proteins are recognized as BCP inhibitors (33). Altogether, these NTA results confirmed the formation of physiologically relevant pCPPs, sCPPs and BCPs based on their morphological features, size distribution and chemical content. As a result, these crystals had the physiological characteristics to mimic their impact on an OA-HACs *in vitro* experiment.

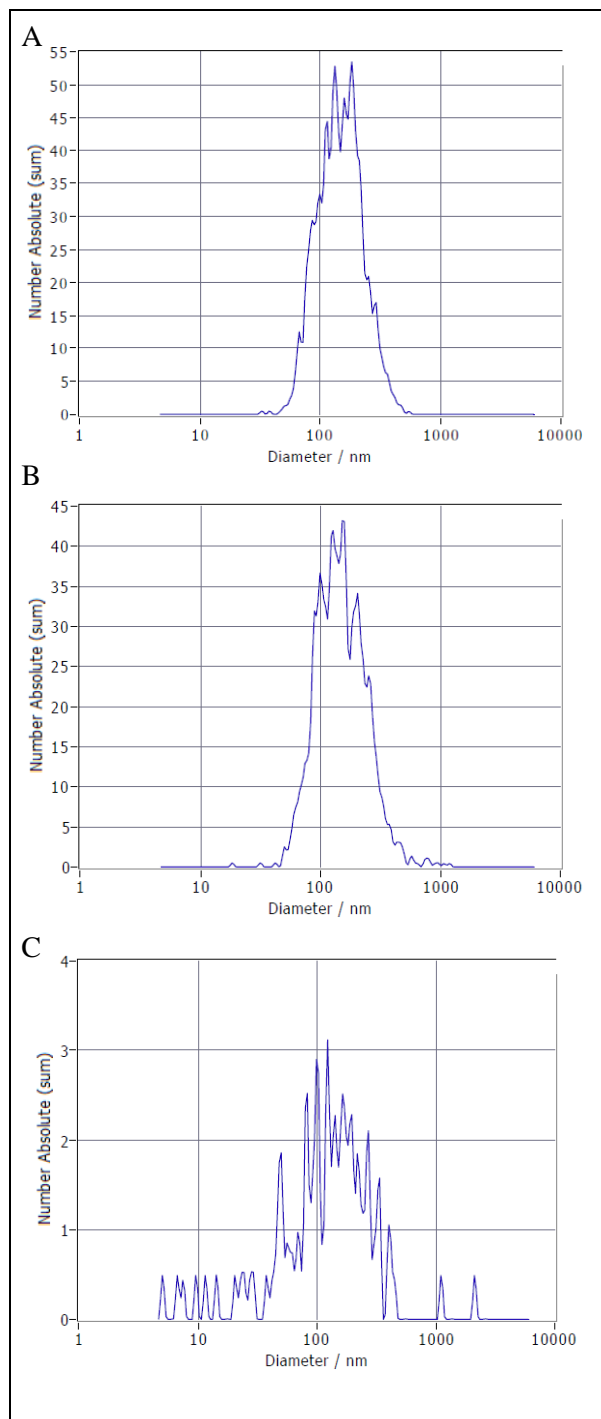


**Figure 4: Particle distribution of pCPP (A), sCPP (B) and BCP (C) measured by NTA.** The NTA measured the size (nm) distribution of the different particles by using light scattering and the Brownian motion within the range of 10nm to 1000nm. NTA, nanoparticle tracking analysis; pCPP, primary calciprotein particle; sCPP, secondary calciprotein particle; BCP, basic calcium phosphate.

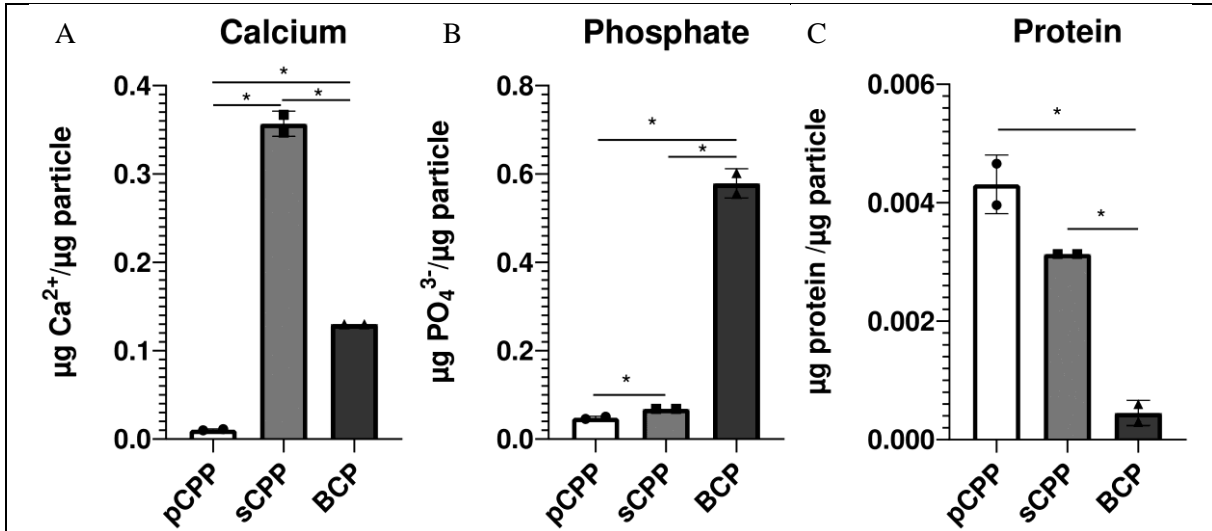


**Figure 5: Measurement of calcium (A), phosphate (B) and protein (C) deposition per particle in calcium-containing particles with colorimetric assays (n=2).** BCP, basic calcium phosphate; pCPP, primary calciprotein particle; sCPP, secondary calciprotein particle.

*The impact of crystals on chondrocytes* – To assess the potential impact of the different crystals on chondrocytes, the responses of an OA-HAC pool (n=6) were evaluated based on cellular behaviour, gene and protein levels. The responses were followed up over 0, 24 and 48 hours and compared to a non-exposed group, to detect changes over time. At first, qualitative images were taken into account to study the cell behaviour after exposure. (Figure 6). The control

conditions of 24 and 48 hours can be compared to the control of 0 hours. After 24 hours, the particles were seen closely in contact with the chondrocytes, resulting in stretching patterns of the cells. After 48 hours, the cells became more elongated in comparison to the control. The particles seem to be dense at 48 hours, probably as a result of maturation and agglomeration over time. These images hinted at the stress response of the OA-HACs to the particles.

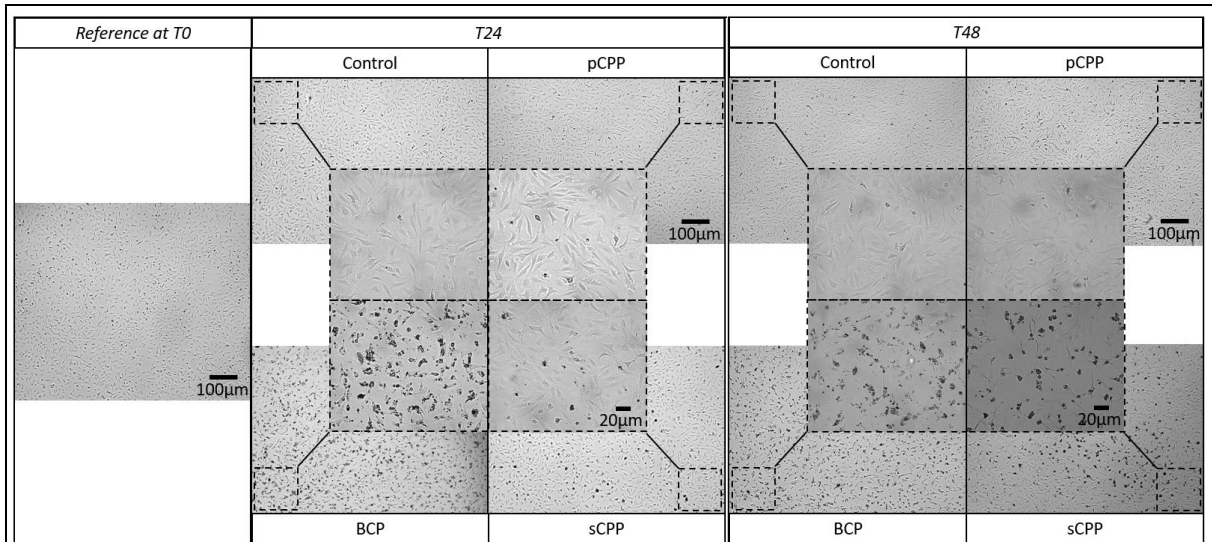


**Figure 6: Qualitatively assessment of human articular chondrocyte responses to BCP, pCPP and sCPP after 0, 24 and 48 hours.** At first, the cell pool of human OA-chondrocytes (n=6) was seeded at a density of 30.000 cells/cm<sup>2</sup> and attached for 24 hours before adding the particles. Subsequently, the cells were stimulated with 50µg/mL pCPP, sCPP or BCP. Images were made with a light microscopy at 20 and 100µm. The indicated squares of the 100µm pictures do not correlate with the region indicated at 20µm. T0, 0 hours; T24, 24 hours; T48, 48 hours; BCP, basic calcium phosphate; pCPP, primary calciprotein particle; sCPP, secondary calciprotein particle.

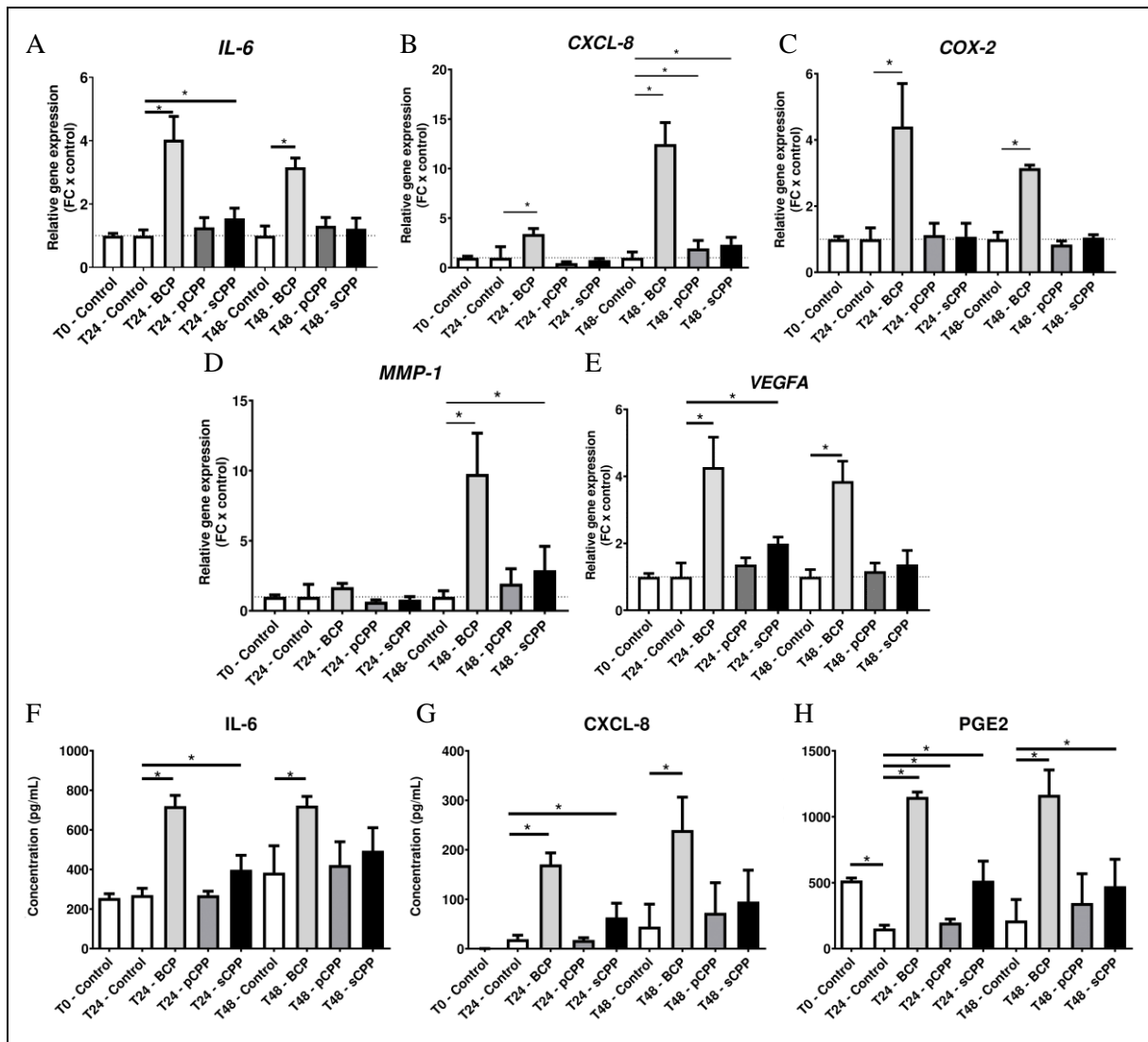


**Figure 7: The responses of OA-HACs at protein and gene level after exposure to BCPs, pCPPs and sCPPs.** A pool of human OA-chondrocytes (n = 6) was stimulated with 50µg/mL BCP, pCPP or sCPP. After 0, 24 and 48 hours of exposure, the gene expression of *IL-6*, *CXCL-8*, *COX-2*, *MMP-1*, *VEGFA* and the protein secretion of *IL-6*, *CXCL-8* and *PGE2* was measured (n<sub>T0,control</sub>=4, n<sub>T24,control</sub>=5, n<sub>T24,BCP-T48,sCPP</sub>=6). **A-E**) The human articular OA chondrocyte gene expression of *IL-6* (A), *CXCL-8* (B), *COX-2* (C), *MMP-1* (D) and *VEGF* (E) was measured with RT-qPCR. **F-H**) Human articular OA chondrocytes secretion levels of *IL-6* (F) and *CXCL-8* (G) were measured with direct enzyme-linked immune sorbent assay, while the secretion of *PGE2* (H) was measured with competitive enzyme-linked immune sorbent assay. The data is represented in bars with mean±SD and is statistically tested with 5% significance value. Statistical analysis was performed with an unpaired Student's *T*-test. The dotted line demonstrates the control of 0, 24 and 48 hours. *IL-6*, interleukin-6; *CXCL-8*, chemokine (C-X-C motif) ligand 8; *COX2*, Cyclo-oxygenase 2; *MMP1*, Matrix Metalloproteinase 1; *VEGFA*, vascular endothelial growth factor type A; *PGE2*, prostaglandin 2; T, hours; FC x control, Fold change compared to the reference gene *Cyclophilin*; \*, P-value.

Furthermore, the impact of pCPP, sCPP and BCP on OA-HACs was studied for gene and protein levels. The pCPP and pCPP responses were less well described in OA, although these particles demonstrated pro-inflammatory responses in endothelial cells (34). The BCP-driven expression and secretion of pro-inflammatory and

cartilage degradable markers were demonstrated in OA-HACs (35). Therefore, pro-inflammatory markers were studied after exposure to pCPPs, sCPPs and BCPs. The gene expression of pro-inflammatory genes *IL-6*, *CXCL-8*, together with *COX-2*, another pro-inflammatory marker, *MMP-1*, a marker of cartilage degradation was

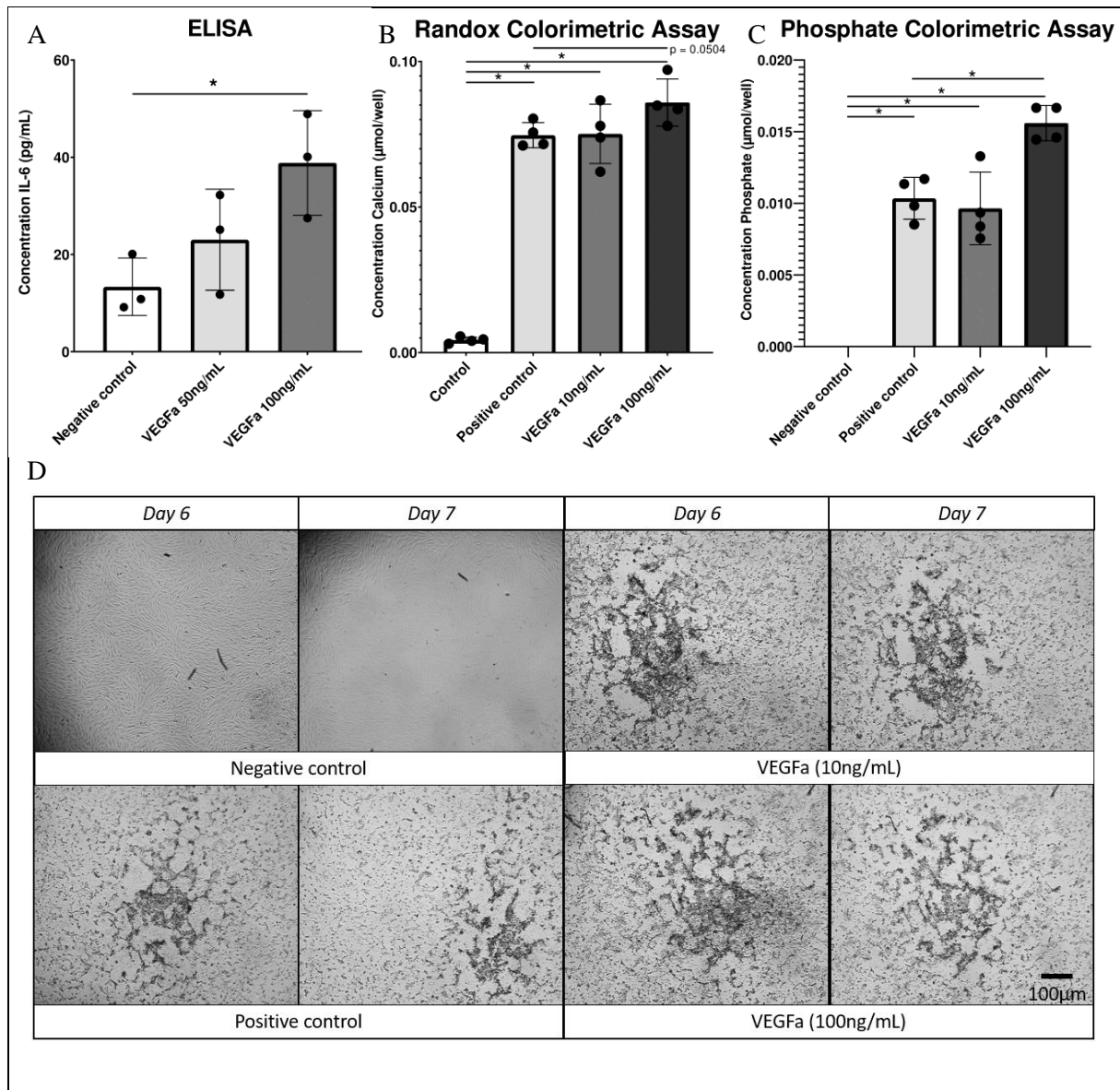


**Figure 8: Exposure of VEGFa on chondrocytes.** **A)** The bioactivity of VEGFa in C28I2 cell line (n = 3). A concentration of 50 and 100ng/mL of VEGFa was administered to assess the bioactivity of VEGFa on C28I2 cells. The protein secretion of pro-inflammatory factor IL-6 demonstrated a significant difference at a concentration of 100ng/mL VEGFa compared to the negative control (n=3). **B-D)** A pool of human OA-chondrocytes (n = 8) was included in a PI model and stimulated with 10 and 100ng/mL VEGFa. The Randox colorimetric assay measured the calcium concentration (**B**). The colorimetric assays measured the calcium and phosphate concentration (n=4) (**C**). Qualification of the OA-HAC-pool at days 6 and 7 with light microscopy at 100μm (**D**). VEGFa, Vascular Endothelial Growth Factor type a; IL-6, interleukin 6. Statistical analysis was performed with an unpaired Student's *T*-test. \*P < 0.05.

measured (Figure 7A-D). The *IL-6* expression significantly increased by 3.03-fold after 24 hours and 2.16-fold after 48 hours of BCP exposure, and also, 0.54-fold in response to sCPP after 24 hours (Figure 7A-B). The expression of *CXCL-8* was significantly increased by 2.40-fold after 24 hours and 11.50-fold after 48 hours of BCP exposure. Also, *CXCL-8* was significantly

increased 0.94-fold and 1.30-fold after 48 hours of exposure to pCPP and sCPP, respectively (Figure 7B). *COX-2* was significantly increased by 3.40-fold after BCP exposure after 24 hours and 2.14-fold after 48 hours, while *MMP1* was significantly increased by 8.76-fold after BCP and 1.89-fold after SCPP at 48 hours (Figure 7C-D). Additionally, since VEGF was demonstrated

to be increased in OA, the angiogenic markers *VEGFA*, *VEGFR1* and *VEGFR2* were measured (21). The angiogenic mediator, *VEGFA*, was significantly increased 2.33-fold after 24 hours, 4.22-fold after 48 hours of BCP exposure and 1.79-fold after 24 hours of sCPP exposure. However, the gene expressive analysis of *VEGFR1* and *VEGFR2* failed to demonstrate any significant differences and was shown in Supplementary Figure 1. Moreover, secreted levels of IL-6 had the same pattern as for *IL-6* expression (Figure 7F). After 24 and 48 hours of exposure to BCP, IL-6 secretions increased to 720pg/mL with a fold change of 1.88. Also, after 24 hours of exposure to sCPP, the secretions of IL-6 increased to 400pg/mL. The CXCL-8 secretions were also significantly increased after 24 and 48 hours of BCP exposure, and 24 hours of exposure to sCPP, with a 7.78, 4.37 and 1.13-fold change respectively (Figure 7G). The pro-inflammatory marker PGE2 demonstrated a significant increase in secretion after exposure to BCP and sCPP after 24 and 48 hours, but also to pCPP after 24 hours of exposure, with a 6.52, 0.29, 0.18, 0.25 and 2.3 fold change, respectively (Figure 7H). These results demonstrated a response in the inflammatory, matrix degradation and angiogenesis level after exposure to the different particles. Moreover, differences in gene and protein levels were more triggered after exposure to BCPs, in comparison to pCPPs and to sCPPs. More responses were demonstrated to sCPPs than for pCPPs. This data confirmed the expected BCP-driven inflammation but indicated new insights on the impacts of BCP on angiogenic markers, such as *VEGFA*. Furthermore, these data indicated the role of pCPP and sCPP in inflammation.

*The impact of VEGF on OA chondrocytes*  
 – Our previous results, indicated a significant increase of *VEGFA* expression in OA-HACs after exposure to sCPPs and BCPs. Furthermore, VEGF had been demonstrated in high concentrations of in OA synovial fluid, compared to the general population (21). Therefore, growth factor VEGF was studied as an inducer of crystal formation and mineralization in an OA-HAC pool (n=8). Firstly, the bioactivity of VEGFa was demonstrated for the IL-6 protein with ELISA, which was significantly increased with a fold change of 1.90 in C28I2 cells compared to the control group (Figure 8A). The secretion of IL-6 increased to 388pg/mL indicating the bio-activity of VEGFa in chondrocytes. Since, VEGFa was

demonstrated to be bio-active in chondrocytes, VEGFa was studied as an inducer of mineralization in an OA-HAC pool (pool n = 8). The PI-OA-HAC model demonstrated a border line significant increase of calcium concentration for 100ng/ml VEGFa compared to the control (Figure 8B). However, the phosphate colorimetric assay demonstrated a significant increase of phosphate concentrations after exposure to 100ng/mL of VEGFa. Both differences in calcium and phosphate concentrations indicate an increase in crystal formation in the presence of 100ng/ml of VEGFa. Furthermore, a qualitative assessment of crystal formation was performed after days 6 and 7 of exposure (Figure 8D). In the negative control, the phosphate donors ATP and BGP were absent, resulting in no crystal formation, while crystal formation was present in the positive control. Comparing the positive control to the conditions of 10 and 100ng/mL VEGFa, indicated the mineralization capacity of VEGFa in OA-HACs. After 7 days of exposure, the amount of empty locations increase in addition of VEGFa 10 and 100ng/mL suggesting a negative impact of the crystals on the cell's survival. VEGF had been indicated as having a role in OA, however, these results were the first to confirm VEGF as an inducer of mineralization of OA-HACs.

## DISCUSSION

The aberrant chondrocyte phenotype is considered a driver of the mineralization of articular cartilage in OA. However, it is unclear which factors induce the loss of chondrocyte phenotypic integrity that leads to the pathological formation of these crystals. Calcium-containing particles are found in OA, but it is unknown whether this is an initiator or a result of the pathology (23). Furthermore, which factors induce mineralization in the OA articular cartilage, is still under debate. Therefore, we aim to study the responses of chondrocytes to calcium-containing particles and the potential influence of growth factors, such as VEGF, in the mineralization capacity of these cells.

We generated physiologically relevant calcium-containing particles, which were confirmed by their morphological features, average size and chemical composition. The pCPPs were perfectly spherical, while sCPPs lost the spherical conformation and demonstrated the presence of protrusions. The BCPs exhibited a crystalline structure of rods. The TEM images for pCPP and sCPP aligned with the generation of

CPP particles described in calcified vascular smooth muscle cells (30). Although compared to the previous study, the sCPPs in our experiment were not abundantly covered with protrusions. Suggesting, that the sCPPs were less mature to their physiological morphological structure as a possible result of inadequate concentrations of calcium, phosphate, proteins or incubation time. Matured TEM images of HA demonstrated the same crystallinity formation in studies characterizing the HAs, which is part of the heterogenous group of BCPs (36, 37). The size distribution of the different particles was measured with NTA, which demonstrated an average size of 144.5nm for pCPP, 143.3nm for sCPP and 123.2nm for BCP. These crystals fall within the same size range of particles prepared for comparative studies, 80-250nm for CPPs and 100-300nm for BCPs (31, 32). Also, chemical characterization was performed for calcium, phosphate and protein contents. The same difference in deposition of calcium and phosphate contents was verified in pCPP and sCPP generated in a calcification study for vascular smooth muscle cells (30). Furthermore, it has been reported that the presence of proteins, such as fetuin-A, is necessary to form pCPPs and sCPPs. Although, fetuin-A has been demonstrated as a direct prevention of pCPP and sCPP precipitation into crystalline HAs (33). The study also reported the spontaneous formation of BCPs in the absence of proteins. Since proteins are considered as a formation inhibitor of BCP, this suggests the low concentrations of proteins in BCP, compared to pCPP and sCPP, in our results. However, the measurement of protein contents in pCPP and sCPP is unexpected, since the CPPs were prepared with only calcium and phosphate in the absence of FCS. The overall findings confirmed the formation of physiologically relevant calcium-containing crystals and hinted towards the conversion of pCPP and sCPP to BCPs by ripening over time. Altogether, these results indicated that the different calcium-containing particles were able to mimic the physiological responses of OA-HACs.

These physiologically relevant BCPs and CPPs were studied for their impact on OA-HACs. The majority of chondrocyte's gene and protein changes were a result of BCP exposure with an effect on pro-inflammatory factors, ECM degrading proteins and angiogenic mediators. In comparison to our results, equal differences were found in IL-6 and MMP1 expression and secretion patterns in Stassen *et al.* (35). However,

the expression pattern of *MMP-1* was not significantly increased after 48 hours in comparison with this study. Moreover, the expression patterns of pro-inflammatory markers, *COX-2* and *CXCL-8*, were significantly increased after exposure to BCP for both 24 and 48 hours. This was also demonstrated for the angiogenic factor *VEGFA*. Nevertheless, these genes were not measured before in OA-HACs exposed to BCPs. Since most of the elevations are induced by BCPs, compared to pCPPs and sCPPs, the BCPs demonstrated to have the largest impact on OA-HACs. This could be the result of their morphological features, in which the TEM images demonstrated the spikey protrusions at their surface able to penetrate the chondrocyte's membrane. This stress-induced penetration could lead to differential expression of pro-inflammatory genes. Fewer effects were seen for pCPPs, except for the *CXCL-8* expression after 48 hours, in comparison to sCPPs. The sCPPs demonstrated significant increases for *IL-6*, *CXCL-8* and *MMP1* expressions. Since sCPP has been suggested as a precursor of BCPs, it was estimated that these sCPPs would react in almost the same manner, although, in a less reactive way than the matured BCPs. Together with the Posner clusters, the pCPP is the initial particle type that forms in the crystal formation sequence, resulting in less characterization and penetrating capacity compared to the more matured types, such as sCPP and BCP. Therefore, they were suggested to have less impact on gene and protein levels of OA-HACs. However, sCPPs are precursors of BCPs, therefore they initiate the formation of protrusions indicating a possible role in impacting the gene and protein levels. The secretion pattern of IL-6 was the same for the different exposure, while *CXCL-8* demonstrated some differential secretions. However, this could be the result of translational mechanisms in the cell. Also, the secretion of PGE2 was measured since the secretion was indicated to be amplified after BCP exposure in human fibroblasts (38). Moreover, Morgan *et al.*, demonstrated that an increase in *COX-2* expression is linked with an increase in PGE2 production after BCP exposure. However, the secretion pattern of PGE2 was more diversely increases compared to the *COX-2* expression. Overall, these results indicated the impact of the different calcium-containing particles on OA-HACs phenotype. Due to CPP induction, the pathways of pro-inflammatory markers, degradation proteins and angiogenic mediators were increased in expression and secretion

pattern. This suggests the role of CPPs in the induction of pro-inflammatory aberrant phenotype of chondrocytes

This study suggested that this CPP-induced aberrant phenotype favours hypertrophy and mineralization. However, less is known about the potential inducers of mineralization by chondrocytes. The previous experiment demonstrated that the gene expression of *VEGFA* was increased after BCP and sCPP exposure. Therefore, VEGFa was suggested as an inducer of mineralization in OA. The possible role of VEGF in OA was also indicated by the increased VEGF/VEGFR expression in chondrocytes of mature OA articular cartilage, while this tissue is normally devoted of angiogenesis (21). Therefore, VEGFa was exposed to a PI-OA-HAC model and demonstrated a significant increase in phosphate deposition. Also, an increase in calcium deposition was found, however, this was not significantly different. Although Faehling *et al.* reported that VEGFa induced an increase of intracellular calcium in endothelial cells (39). Less is studied about the impact of VEGFa on phosphate channels, demonstrating that VEGFa activity is primarily based on calcium concentrations, but this is only discussed in studies about angiogenesis. Nevertheless, these results indicate that VEGFa is an inducer of phosphate-deposited mineralization in OA-HACs and therefore a possible inducer of crystal formation.

Also, the study has some limitations. Since most of the experiments are performed once, the results are derived from a one-point measurement. This was prevented by using multiple measurements of the same sample. However, these samples still have the same origin. Therefore, these experiments should be repeated with different samples to validate the data, which can lead to new insights. Also, patient-dependent variation is important. During this study, two OA-HAC pools were used to perform the experiments, resulting from 14 patients. It would be interesting to perform these experiments on more different OA-HAC pools to increase the heterogeneity further. Although, most of the OA-HAC pools were developed to induce patient variability. Additionally, chondrocytes in cultures are tended to dedifferentiate into fibroblasts during subculturing (40). Furthermore, the culture media or environment where the cells are cultured in can impact their phenotype. Therefore, it is important to minimize the number of passages. In this study,

this was limited by using the cells at the second passage. Moreover, the culture conditions were standardized to mimic the physiological environment and prevent this dedifferentiation as much as possible. In future perspectives, it would be interesting to elaborate on the impacts of calcium-containing growth factors on more genes and proteins, such as different MMPs for demonstrating further the cartilage degeneration. Furthermore, inhibition of phosphate and calcium channels in mineralization would give more insights into how the VEGF mineralization by OA-HACs is induced. Also, studying the inhibitions of phosphate and calcium channels in different OA isolates, differing in BMI, gender and age. Finally, investigating the effects of other growth factors on the mineralization of OA-HACs.

In conclusion, our data indicated that pCPP, sCPP and BCP crystals induce inflammation and angiogenesis in OA-HACs and that VEGFa is an inducer of cartilage mineralization in OA. Further investigation is necessary to determine the mechanism behind the role of VEGFa in mineralization and the mechanisms behind the different pro-inflammatory profiles. This could aid in the development of new therapeutic insights.

## CONCLUSION

The aberrant chondrocyte phenotype is induced by the presence of pCPP, sCPP and BCP affecting the expressions and secretions of pro-inflammatory proteins, degradation proteins and angiogenic factors. One of the angiogenic factors, VEGFa, induces the phosphate-deposited mineralization of OA-HACs.

*Acknowledgements* – I would like to express my gratitude to the members of the Laboratory for Experimental Orthopedics at Maastricht University for providing me with valuable experience in performing experiments in a biomedical research lab. I am grateful for the opportunity to be part of such an exceptional team dedicated to research in osteoarthritis. Also, I would like to thank Mr Msc. Roderick Stassen (RS), my daily promotor, for his guidance and support throughout my internship. His expertise and constructive feedback have been instrumental in understanding the theoretical fundamentals and enhancing of my lab skills. I am truly grateful for his patience, generosity, and willingness to share his knowledge. Furthermore, I want to thank Dr Guus Van Den Akker (GA) for the opportunity to study, learn and grow during my internship.

*Author contributions* – RS and GA designed the research goals. I performed the experiments and data analysis, under the supervision of my promotor. I wrote the paper with feedback from my promotor and supervisor. All authors carefully edited the manuscript.

SUPPLEMENTARY

**Table 1: Characteristics of patients used in the OA-HAC pools. M, male; F, female; BMI, Body Mass Index.**

OA-HAC pool (n=6)			OA-HAC pool (n=8)		
M/F	BMI (kg/m <sup>2</sup> )	Age (years)	M/F	BMI (kg/m <sup>2</sup> )	Age (years)
F	69	30,1	F	29,9	81
F	75	30,1	F	25,7	60
F	75	27,6	F	31,2	73
F	23	38,6	F	25,5	74
M	72	30,4	M	23,9	59
M	58	34,6	M	29,4	82
			M	26,4	74
			M	31,4	72
Average	62	31.9	Average	29	72

**Table 2 – qPCR primers.** These primers were diluted 5 times of 100µM stock.

Type of gene	Name primer	Gene sequence
Reference	Cyclophiline ( <i>hcylo</i> )	Forward 5'- TTC-CTG-CTT-TCA-CAG-AAT-TAT-TCC -3'
		Reverse 5'- GCC-ACC-AGT-GCC-ATT-ATG-G -3'
Inflammation	Human interleukine 6 ( <i>hIL-6</i> )	Forward 5'- TGT-AGC-CGC-CCC-ACA-CA -3'
		Reverse 5'- GGA-TGT-ACC-GAA-TTT-GTT-TGT-CAA -3'
	Human chemokine (C-X-C motif) ligand 8 ( <i>hCXCL-8</i> )	Forward 5'- TGCTAGCCAGGATCCACAAGT -3'
		Reverse 5'- TGTGAGGTAAGATGGTGGCTAATACT -3'
	Human Cyclooxygenase ( <i>hCOX-2</i> )	Forward 5'- ACC-AAC-ATG-ATG-TTT-GCA-TTC-TTT -3'
		Reverse 5'- GGT-CCC-CGC-TTA-AGA-TCT-GTC-T -3'
	Human Metalloproteinase 1 ( <i>hMMP-1</i> )	Forward 5'- GATGGACCTGGAGGAAATCTTG -3'
		Reverse 5'- TGAGCATCCCCTCCAATACC -3'
Angiogenesis	Human Vascular endothelial growth factor type A ( <i>hVEGFA</i> )	Forward 5'- GGCAGAAATCATCACGAAGTG -3'
		Forward 5'- GTCCACCAGGGTCTCGATTG -3'
	Human Vascular endothelial growth factor receptor 1 ( <i>hVEGFR1</i> )	Reverse 5'- CAGAATCCTCCTCTTCCTCAACAT -3'
		Reverse 5'- CAGAATCCTCCTCTTCCTCAACAT -3'
	Human Vascular endothelial growth factor receptor 2 ( <i>hVEGFR2</i> )	Forward 5'- CACCACTCAAACGCTGACATGTA -3'
		Reverse 5'- CGTTGGCGCACTCTCCT -3'

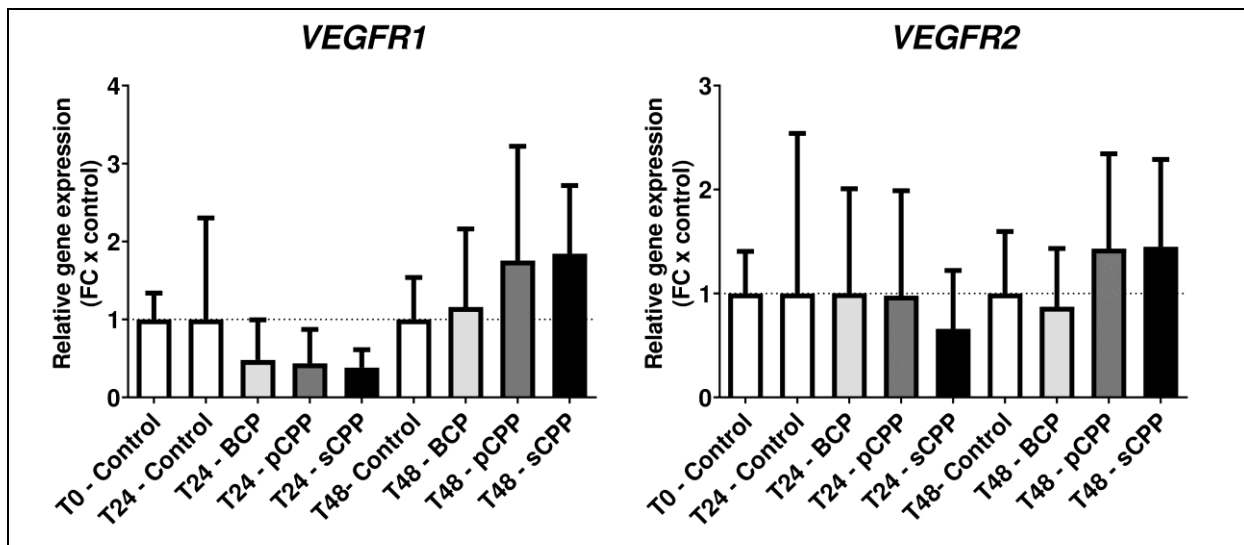


**Figure 1: The responses of OA-HACs at protein and gene level after exposure to BCPs, pCPPs and sCPPs for VEGFR1 (A) and VEGFR2 (B).** A pool of human OA-chondrocytes (n = 6) was stimulated with 50µg/mL BCP, pCPP or sCPP. After 0, 24 and 48 hours of exposure, the gene expression of VEGFR1 and VEGFR2 was measured. The data is represented in bars with mean±SD and is statistically tested with 5% significance value. Statistical analysis was performed with unpaired Student’s T-test. The dotted line demonstrates the control of 0, 24 and 48 hours. VEGFR1-2, Human Vascular endothelial growth factor receptor 1-2. T, hours; FC x control, Fold change compared to the reference gene Cyclophilin; \*, P-value.

## REFERENCES

1. Beasley J. Osteoarthritis and rheumatoid arthritis: conservative therapeutic management. *Journal of hand therapy : official journal of the American Society of Hand Therapists*. 2012;25(2):163-71; quiz 72.
2. Felson DT. Clinical practice. Osteoarthritis of the knee. *N Engl J Med*. 2006;354(8):841-8.
3. He Y, Li Z, Alexander PG, Ocasio-Nieves BD, Yocum L, Lin H, et al. Pathogenesis of Osteoarthritis: Risk Factors, Regulatory Pathways in Chondrocytes, and Experimental Models. *Biology*. 2020;9(8).
4. Taruc-Uy RL, Lynch SA. Diagnosis and treatment of osteoarthritis. *Primary care*. 2013;40(4):821-36, vii.
5. Musumeci G, Aiello FC, Szychlinska MA, Di Rosa M, Castrogiovanni P, Mobasher A. Osteoarthritis in the XXIst century: risk factors and behaviours that influence disease onset and progression. *International journal of molecular sciences*. 2015;16(3):6093-112.
6. OARSI White paper - Osteoarthritis: A Serious Disease. *Osteoarthritis research society international*. 2016.
7. Abramoff B, Caldera FE. Osteoarthritis: Pathology, Diagnosis, and Treatment Options. *The Medical clinics of North America*. 2020;104(2):293-311.
8. Cross M, Smith E, Hoy D, Nolte S, Ackerman I, Fransen M, et al. The global burden of hip and knee osteoarthritis: estimates from the global burden of disease 2010 study. *Annals of the rheumatic diseases*. 2014;73(7):1323-30.
9. Long H, Liu Q, Yin H, Wang K, Diao N, Zhang Y, et al. Prevalence Trends of Site-Specific Osteoarthritis From 1990 to 2019: Findings From the Global Burden of Disease Study 2019. *Arthritis & rheumatology (Hoboken, NJ)*. 2022;74(7):1172-83.
10. Hawker GA. Osteoarthritis is a serious disease. *Clinical and experimental rheumatology*. 2019;37 Suppl 120(5):3-6.
11. Amoako AO, Pujalte GG. Osteoarthritis in young, active, and athletic individuals. *Clinical medicine insights Arthritis and musculoskeletal disorders*. 2014;7:27-32.
12. Sophia Fox AJ, Bedi A, Rodeo SA. The basic science of articular cartilage: structure, composition, and function. *Sports health*. 2009;1(6):461-8.
13. Ulrich-Vinther M, Maloney MD, Schwarz EM, Rosier R, O'Keefe RJ. Articular cartilage biology. *The Journal of the American Academy of Orthopaedic Surgeons*. 2003;11(6):421-30.
14. Tuan RS, Chen AF, Klatt BA. Cartilage regeneration. *The Journal of the American Academy of Orthopaedic Surgeons*. 2013;21(5):303-11.
15. Conway R, McCarthy GM. Calcium-Containing Crystals and Osteoarthritis: an Unhealthy Alliance. *Current rheumatology reports*. 2018;20(3):13.
16. Kronenberg HM. Developmental regulation of the growth plate. *Nature*. 2003;423(6937):332-6.
17. SF G. *Osteogenesis: Developmental Biology*. Sinauer Associates. 2000(Chapter 14).
18. Berendsen AD, Olsen BR. Bone development. *Bone*. 2015;80:14-8.
19. Dreier R. Hypertrophic differentiation of chondrocytes in osteoarthritis: the developmental aspect of degenerative joint disorders. *Arthritis research & therapy*. 2010;12(5):216.
20. van der Kraan PM. Differential Role of Transforming Growth Factor-beta in an Osteoarthritic or a Healthy Joint. *Journal of bone metabolism*. 2018;25(2):65-72.

21. Murata M, Yudoh K, Masuko K. The potential role of vascular endothelial growth factor (VEGF) in cartilage: how the angiogenic factor could be involved in the pathogenesis of osteoarthritis? *Osteoarthritis and cartilage*. 2008;16(3):279-86.
22. Fuerst M, Niggemeyer O, Lammers L, Schäfer F, Lohmann C, Rütter W. Articular cartilage mineralization in osteoarthritis of the hip. *BMC musculoskeletal disorders*. 2009;10:166.
23. Stücker S, Bollmann M, Garbers C, Bertrand J. The role of calcium crystals and their effect on osteoarthritis pathogenesis. *Best practice & research Clinical rheumatology*. 2021;35(4):101722.
24. Yan JF, Qin WP, Xiao BC, Wan QQ, Tay FR, Niu LN, et al. Pathological calcification in osteoarthritis: an outcome or a disease initiator? *Biological reviews of the Cambridge Philosophical Society*. 2020;95(4):960-85.
25. Roohani I, Cheong, S., & Wang, A. How to build a bone? - Hydroxyapatite or Posner's clusters as bone minerals. *Open Ceramics*. 2021.
26. Smith ER, Hewitson TD, Jahnen-Dechent W. Calciprotein particles: mineral behaving badly? *Current opinion in nephrology and hypertension*. 2020;29(4):378-86.
27. Heiss A, Eckert T, Aretz A, Richtering W, van Dorp W, Schäfer C, et al. Hierarchical role of fetuin-A and acidic serum proteins in the formation and stabilization of calcium phosphate particles. *The Journal of biological chemistry*. 2008;283(21):14815-25.
28. Timur UT, Jahr H, Anderson J, Green DC, Emans PJ, Smagul A, et al. Identification of tissue-dependent proteins in knee OA synovial fluid. *Osteoarthritis and cartilage*. 2021;29(1):124-33.
29. Ea HK, Chobaz V, Nguyen C, Nasi S, van Lent P, Daudon M, et al. Pathogenic role of basic calcium phosphate crystals in destructive arthropathies. *PloS one*. 2013;8(2):e57352.
30. Aghagolzadeh P, Bachtler M, Bijarnia R, Jackson C, Smith ER, Odermatt A, et al. Calcification of vascular smooth muscle cells is induced by secondary calciprotein particles and enhanced by tumor necrosis factor- $\alpha$ . *Atherosclerosis*. 2016;251:404-14.
31. Ewence AE, Bootman M, Roderick HL, Skepper JN, McCarthy G, Epple M, et al. Calcium Phosphate Crystals Induce Cell Death in Human Vascular Smooth Muscle Cells. *Circulation Research*. 2008;103(5):e28-e34.
32. Miura Y, Iwazu Y, Shiizaki K, Akimoto T, Kotani K, Kurabayashi M, et al. Identification and quantification of plasma calciprotein particles with distinct physical properties in patients with chronic kidney disease. *Scientific reports*. 2018;8(1):1256.
33. Pasch A, Farese S, Gräber S, Wald J, Richtering W, Floege J, et al. Nanoparticle-based test measures overall propensity for calcification in serum. *Journal of the American Society of Nephrology : JASN*. 2012;23(10):1744-52.
34. Shishkova D, Lobov A, Zainullina B, Matveeva V, Markova V, Sinitskaya A, et al. Calciprotein Particles Cause Physiologically Significant Pro-Inflammatory Response in Endothelial Cells and Systemic Circulation. *International journal of molecular sciences*. 2022;23(23).
35. Stassen R, van den Akker GGH, Surtel DAM, Housmans BAC, Cremers A, Caron MMJ, et al. Unravelling the Basic Calcium Phosphate crystal-dependent chondrocyte protein secretome; a role for TGF- $\beta$  signaling. *Osteoarthritis and cartilage*. 2023.
36. al Te. Evolution of Amorphous Calcium Phosphate to Hydroxyapatite Probed by Gold Nanoparticles. *Journal of Physical Chemistry C*. 2008.

37. Watanabe KN, Ikuko & Imai, Hiroaki. Dispersion of hydroxyapatite nanocrystals stabilized by polymeric molecules bearing carboxy and sulfo groups. *Colloid and Polymer Science*. 2017.
38. Morgan MP, Whelan LC, Sallis JD, McCarthy CJ, Fitzgerald DJ, McCarthy GM. Basic calcium phosphate crystal-induced prostaglandin E2 production in human fibroblasts: role of cyclooxygenase 1, cyclooxygenase 2, and interleukin-1beta. *Arthritis and rheumatism*. 2004;50(5):1642-9.
39. Faehling M, Koch ED, Raithel J, Trischler G, Waltenberger J. Vascular endothelial growth factor-A activates Ca<sup>2+</sup>-activated K<sup>+</sup> channels in human endothelial cells in culture. *The international journal of biochemistry & cell biology*. 2001;33(4):337-46.
40. Gosset M, Berenbaum F, Thirion S, Jacques C. Primary culture and phenotyping of murine chondrocytes. *Nature protocols*. 2008;3(8):1253-60.